

## Magnetic ordering in CsCoBr<sub>3</sub>

W. B. Yelon\*†

*Institut Laue-Langevin, B.P. 156, 38042 Grenoble Cedex, France*

D. E. Cox\*

*Brookhaven National Laboratory, Upton, New York 11973*

M. Eibschütz

*Bell Laboratories, Murray Hill, New Jersey 07974*

(Received 31 March 1975)

The magnetic ordering in CsCoBr<sub>3</sub> has been studied by neutron diffraction, on both powder and single-crystal specimens, and by specific-heat and magnetic-susceptibility measurements. This compound has the hexagonal CsNiCl<sub>3</sub> type of structure, and the susceptibility shows characteristic one-dimensional behavior, while the specific heat indicates that three-dimensional ordering occurs at about 28°K. The neutron single-crystal study shows that between  $T_N$  and 14°K the magnetic structure is consistent with the orthorhombic space group  $Cmc2_1$ , with one-third of the antiferromagnetic cobalt chains being disordered and the other two-thirds antiferromagnetically coupled in the basal plane. Between 4 and 10°K the structure may be described by the space group  $Cm'c2_1'$ , and is similar to the collinear arrangement reported for CsCoCl<sub>3</sub> and RbCoBr<sub>3</sub> but with a small canting of about 10°. The transformation from one structure to the other in the region of 10–14°K can be explained equally well by either the formation of an intermediate phase of lower symmetry or by a discontinuous process in which the two phases coexist. The powder data reveal a small amount of a second low-temperature phase compatible with the space  $C_p m' c 2_1'$ , consistent with negative rather than positive next-nearest-neighbor interactions in the basal plane.

### I. INTRODUCTION

The hexagonal  $ABX_3$  double halides, in which  $A$  is Cs or Rb, constitute an interesting group of magnetic materials. A notable feature of these materials is that the exchange interactions along  $c$ -axis chains of  $3d$  ions are much stronger than those in the basal plane. The systems consequently exhibit one-dimensional magnetic behavior characterized by significant correlations along the  $c$ -axis chains at temperatures 3–10 times higher than the ordering temperature, depending on the compound.<sup>1</sup>

Because of the weak basal-plane interactions and the competition with anisotropy forces, as well as the instabilities associated with antiferromagnetic order in a hexagonal net, the magnetic behavior of these compounds tends to be quite complicated in the ordered phase. Most of the materials studied by neutron scattering have contained either Ni or Mn,<sup>2–4</sup> and the anisotropy has been quite small. The present study deals with CsCoBr<sub>3</sub>, where the anisotropy might be expected to play a major role. CsCoBr<sub>3</sub> is well suited for neutron studies, having small absorption and incoherent-scattering cross sections. In addition, the material orders at 28.3°K, a relatively high temperature for these systems. Our data reveal that the ordering in CsCoBr<sub>3</sub> is quite complicated, in that initially only two-thirds of the cobalt chains order three dimensionally. Ordering of the remaining one-third takes place at a lower temperature

via a rather unusual type of magnetic transition. A recent neutron-diffraction study of CsCoCl<sub>3</sub> has revealed a collinear structure at 4.2°K similar to the low-temperature structure we report here.<sup>5</sup> The temperature dependence of the magnetic intensities in CsCoCl<sub>3</sub> is quite complicated, and the magnetic structure near  $T_N$  is different from the low-temperature structure. It is clear that similar processes are involved in these two materials, but the data for CsCoCl<sub>3</sub> are not sufficient to permit a detailed comparison.

### II. EXPERIMENTAL DETAILS

As far as we are aware, CsCoBr<sub>3</sub> has not previously been reported in the literature. A sample was prepared by careful evaporation of a solution of cesium carbonate (Cs<sub>2</sub>CO<sub>3</sub>) and cobalt carbonate in HBr. The dried powder was maintained at 500°C (just above the melting point) in an atmosphere of anhydrous HBr for 2 h. The resulting product, which was green and very hygroscopic, was handled in a glove bag filled with dry helium gas. An x-ray powder photograph showed a single hexagonal phase of CsNiCl<sub>3</sub> type with lattice constants  $a = 7.52_9$  Å and  $c = 6.32_4$  Å. A single crystal was grown from the melt from part of this material by the Bridgman technique. Chemical analysis gave Cs 30.9 wt% (30.8), Co 13.4 wt% (13.7), Br 55.6 wt% (55.5), the theoretical weight percentages being given in parentheses.<sup>6</sup>

The magnetic susceptibility (Fig. 1) of the material is quite similar to that of CsCoCl<sub>3</sub> as mea-

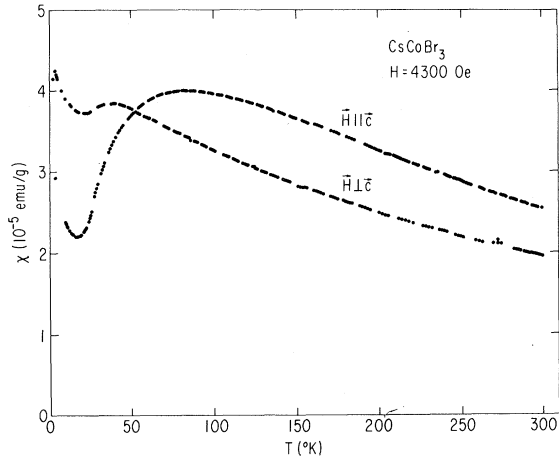


FIG. 1. Magnetic susceptibility of a single crystal of  $\text{CsCoBr}_3$  as a function of temperature. The broad peak in the parallel component is typical of one-dimensional magnetic behavior.

sured by Achiwa,<sup>1</sup> showing a broad maximum in the parallel susceptibility at a temperature of about 50 °K and a smaller somewhat sharper peak in the perpendicular component. However, there is no evidence of long-range magnetic order. On the other hand, the specific heat (Fig. 2) shows a well-defined anomaly at about 28 °K characteristic of the onset of three-dimensional ordering.

Powder neutron data were taken at 77 °K, 4.5 °K, and a number of intermediate temperatures with neutrons of 1.03-Å wavelength. Single-crystal data were collected from a small cleaved portion of the Bridgman sample mounted on the (100) cleavage plane in a standard low-temperature crystal holder. The crystal was rather irregular in shape, roughly 2 mm high by 4×2 mm<sup>2</sup> in cross section. Data were collected in the (*hhl*) zone with neutrons of 1.20-Å wavelength at several tempera-

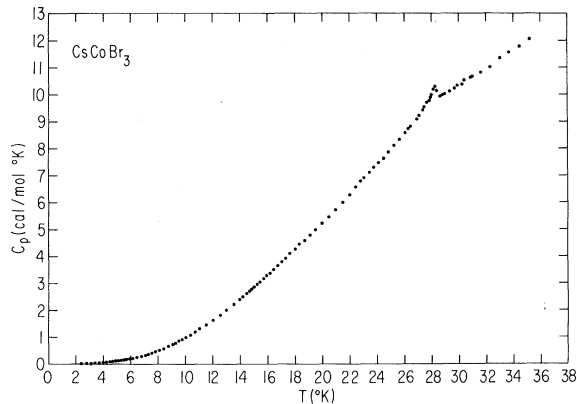


FIG. 2. Specific heat of  $\text{CsCoBr}_3$  as a function of temperature. The Néel point at  $T \approx 28^\circ\text{K}$  is clearly visible, but no anomaly can be seen in the range 10–14 °K.

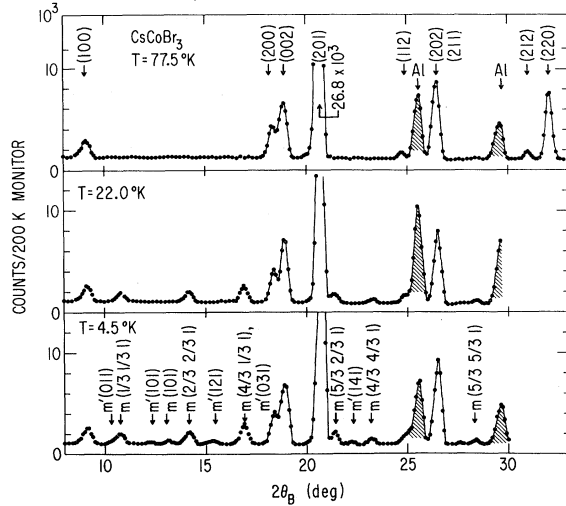


FIG. 3. Powder neutron-scattering data for  $\text{CsCoBr}_3$  at 77.5, 22, and 4.5 °K. The additional peaks at 22 °K are magnetic. At 4.5 °K two sets of magnetic peaks are seen, designated *m* and *m'*, and are due to the coexistence of two related phases. Peaks labeled *m'* are indexed in terms of an orthorhombic cell with dimensions  $a\sqrt{3}$ , *a*, *c*. All others are in terms of the basic hexagonal cell.

tures between 4.3 and 32 °K.

### III. POWDER NEUTRON RESULTS

Intensity data taken at 77, 22, and 4.5 °K are shown in Fig. 3. At 22 °K an additional set of peaks is present which can be indexed on the basis of a hexagonal cell with dimensions  $a\sqrt{3}$ , *c* in terms of the chemical cell, as shown by the broken outline in Fig. 4. The reflection conditions based on the chemical cell<sup>7</sup> are  $h = \frac{1}{3}j$ ,  $k = \frac{1}{3}j'$ ,  $j - j' = 3n$ ,  $j + j' \neq 3n'$ , *l* odd, where *j*, *j'*, *n*, and *n'* are integers. These conditions are identical to those observed in  $\text{CsNiCl}_3$ ,<sup>8</sup> which contains antiferromagnetic *c*-axis chains of moments coupled in a triangular array [Fig. 5(c)]. However, a novel feature in  $\text{CsCoBr}_3$  is the appearance of two more sets of magnetic lines as the temperature is lowered below 16 °K, as seen in the 4.5 °K pattern. One of these sets can be indexed on the basis of the original primitive cell, and in association with the 22 °K set, is characteristic of a collinear, rather than a triangular arrangement, as found, e.g., in  $\text{RbCoBr}_3$  at 4.2 °K [Fig. 5(b)]. The other set, denoted *m'* in Fig. 3, although small, are well above background levels, and can be indexed on the basis of an orthorhombic cell with dimensions  $a\sqrt{3}$ , *a*, *c* in terms of the original hexagonal cell. Orthorhombic reflection conditions in this case are  $h + k$  odd, *l* odd. This cell corresponds to that observed in  $\text{CsNiF}_3$ ,<sup>9</sup> in which adjacent ferromagnetic (110) sheets are coupled antiferromagnetically. However, in  $\text{CsNiF}_3$  there is ferromagnetic coupling

within the chains, and  $l$  is even.

Neglecting the latter set of orthorhombic peaks for the time being, the simplest explanation is that there is a transition from the triangular CsNiCl<sub>3</sub> to the collinear RbCoBr<sub>3</sub> structure at about 15 °K. However, this is clearly untenable from intensity considerations, since quite large changes in intensity ratios would be expected proportional to changes in the magnetic interaction term  $\langle q^2 \rangle$ . The vector  $\vec{q}$  is defined in the usual way as  $\vec{\epsilon}(\vec{\epsilon} \cdot \vec{\kappa}) - \vec{\kappa}$ , where  $\vec{\epsilon}$  and  $\vec{\kappa}$  are unit scattering and spin vectors, respectively, and  $q^2$  is averaged over crystallographically equivalent reflections. The observed values demonstrate that, over the whole temperature range, comparatively little deviation of the moments from the  $c$  axis can be accommodated. In view of this feature, the rather complex temperature dependence, and the presence of some degree of preferred orientation, a detailed single-crystal study was made.

#### IV. SINGLE-CRYSTAL NEUTRON RESULTS

##### A. Nuclear structure refinement

Nuclear intensities were accurately measured at a number of temperatures in order to check for possible crystallographic phase changes accompanying the magnetic ones. At least 17 reflections were measured, and in all cases intensities of equivalent peaks were found to agree to within better than 6%. In the course of these measurements, a smaller twin crystal was seen, having about one-fourth of the volume of the main crystal, but this did not result in any ambiguity. The full width at half-maximum of the rocking curve from the principal portion was found to be about 0.15°.

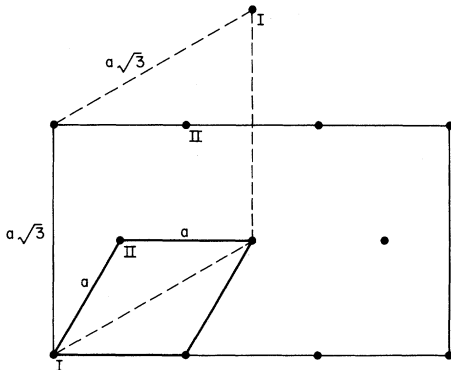


FIG. 4. Basal-plane projection of the chemical and magnetic cells of CsCoBr<sub>3</sub>. The hexagonal cell, dimensions  $a$ ,  $a$ ,  $c$  (heavy lines) is the chemical cell. The tripled  $a\sqrt{3}$ ,  $a\sqrt{3}$ ,  $c$  cell (dashed lines) is the smallest cell consistent with the observed magnetic reflections, while the  $a\sqrt{3}$ ,  $3a$ ,  $c$  orthorhombic cell corresponds to the proposed magnetic structures for both the high- and low-temperature phases.

STRUCTURE	F(h k l)			
	$h = j/3, k = j/3, l = 2n+1$			
	$j, j' = 3n$	$F^2/\rho^2$ $\mu_I^2/\mu_{II}^2$ $q^2=1$	$j, j' \neq 3n$	$F^2/\rho^2$ $\mu_I^2/\mu_{II}^2$ $q^2=1$
a) F (RbCoBr <sub>3</sub> ) 	$F_I = 0$ $F_{II} = 2p(\mu_I + 2\mu_{II})$	0 36	$F_I = 0$ $F_{II} = 2p(\mu_I - \mu_{II})$	0 0
b) B <sub>z</sub> (RbCoBr <sub>3</sub> ) 	$F_I = 0$ $F_{II} = 2p(\mu_I - 2\mu_{II})$	0 4	$F_I = 0$ $F_{II} = 2p(\mu_I + \mu_{II})$	0 16
c) B <sub>x</sub> A <sub>y</sub> (CsNiCl <sub>3</sub> ) 	$F_I = 0$ $F_{II} = 2p(\mu_I - 2\mu_{II} \cos \theta)$	0 $(\theta = 60^\circ)$	$F_I = 2p(i\sqrt{3}\mu_2 \sin \theta)$ $F_{II} = 2p(\mu_I + \mu_2 \cos \theta)$	9 9 $(\theta = 60^\circ)$
d) A <sub>z</sub> (CsCoBr <sub>3</sub> ) 	$F_I = 0$ $F_{II} = 0$	0 0	$F_I = 0$ $F_{II} = 2p(i\sqrt{3}\mu_2)$	0 12
e) A <sub>z</sub> B <sub>y</sub> (CsCoBr <sub>3</sub> ) 	$F_I = 2p(\mu_I - 2\mu_{II} \sin \theta)$ $F_{II} = 0$	0 $(\theta = 30^\circ)$	$F_I = 2p(\mu_I + \mu_2 \sin \theta)$ $F_{II} = 2p(i\sqrt{3}\mu_2 \cos \theta)$	9 9 $(\theta = 30^\circ)$
f) T (CsMnBr <sub>3</sub> ) 	$F_I = 0$ $F_{II} = 0$	0 0	$F_I = 2p(\mu_I + \frac{1}{2}\mu_2 + i\frac{1}{2}\mu_2)$ $F_{II} = 0$	18 0

FIG. 5. Some of the possible magnetic structures for the ABX<sub>3</sub> compounds. Reflection conditions are given in terms of the chemical indices, and structure factors are given for  $j, j' = 3n$  and  $j, j' \neq 3n$ , with form factor and  $q^2$  dependence removed. The contribution due to the components of the moment parallel and perpendicular to  $c$  are linearly independent and are given separately. Special cases with  $\mu_I = \mu_{II}$  are shown.  $p = 0.2695f$ . (a) Ferromagnetic collinear sheets ( $P6_3'/m'cm'$ ). (b) Collinear B<sub>z</sub> structure ( $P6_3'/m'cm'$ ). (c) CsNiCl<sub>3</sub> structure, type B<sub>x</sub>A<sub>y</sub> ( $Cm'c2_1$ ). (d) A<sub>z</sub> structure ( $P6_3'/m'cm'$ ) with disorder on site I. (e) A<sub>z</sub>B<sub>y</sub> structure ( $Cmc2_1$ ). (f) Triangular A<sub>x</sub>B<sub>y</sub> or A<sub>y</sub>B<sub>x</sub> basal-plane structure ( $P\bar{6}2'm'$  or  $P\bar{6}2m$ ).

The intensities of all the nuclear peaks were constant within statistical accuracy over the entire temperature range. The data were corrected for absorption, and least-squares refinements were performed at 4.5, 16, and 32 °K. Extinction effects were quite significant, reducing the intensity of the strongest peak by about 60%, and an extinction parameter was therefore included as a parameter in the fitting procedure. Table I gives the final values for the parameters at the three temperatures. In Table II, the observed and calculated

TABLE I. Parameter values obtained from least-squares refinements of the single-crystal nuclear data from CsCoBr<sub>3</sub>. Standard errors are given in parentheses and refer to the least significant figure(s). Scattering lengths used were  $0.55 \times 10^{-12}$ ,  $0.25 \times 10^{-12}$ , and  $0.679 \times 10^{-12}$  cm for Cs, Co, and Br, respectively.  $R_w = [\sum w(I_{\text{obs}} - I_{\text{calc}})^2 / \sum w(I_{\text{obs}})^2]^{1/2}$ , where  $w$  is the weight assigned to the observed intensity.

	4.5 °K	16 °K	32 °K
Br positional parameter	0.1609(2)	0.1607(1)	0.1610(2)
Extinction factor	843(54)	898(54)	898(81)
Scale factor	5.45(14)	5.66(14)	5.61(20)
Temperature factor ( $\text{\AA}^2$ )	0.28(5)	0.30(5)	0.31(7)
Weighted R factor, $R_w$	0.041	0.040	0.057

TABLE II. Comparison of observed and calculated single-crystal nuclear intensities for CsCoBr<sub>3</sub> at 4.5°K. Parameters as in Table I.

<i>hkl</i>	<i>I</i> <sub>obs</sub>	<i>I</i> <sub>calc</sub>
110	0.8 <sub>3</sub>	0.9 <sub>1</sub>
220	103.9	104.8
330	0.8 <sub>6</sub>	0.7 <sub>3</sub>
440	75.0	75.7
002	142.6	140.4
112	5.6	5.4
222	74.7	78.4
332	1.8	1.9
442	58.6	55.6
004	118.8	116.1
114	0.3 <sub>6</sub>	0.3 <sub>7</sub>
224	85.9	88.8
334	0.5 <sub>5</sub>	0.6 <sub>0</sub>
006	71.1	67.9
116	2.5	2.5
226	58.6	59.1

intensities at 4.5°K are compared. This data set is typical of the entire temperature range. It should be noted that within standard errors the parameters do not vary as a function of temperature, and there is no evidence of any lowering of crystal symmetry connected with the magnetic phase transitions.

#### B. Magnetic data

Magnetic data were collected at several temperatures. The general features of the temperature dependence of the intensities of the magnetic reflections were in agreement with the powder results, with the exception that no peaks characteristic of the  $a\sqrt{3}$ ,  $a$ ,  $c$  orthorhombic cell (Fig. 4) were observed, although a thorough search was made. Below the Néel temperature at about 28°K the neutron data showed peaks of the type (*hhl*), with  $h = \frac{1}{3}j$  and  $l$  odd. Below 14°K, peaks of this type were visible for all integer values of  $j$ , but between 14°K and  $T_N$  only peaks of the type  $j \neq 3n$  were present. Figure 6 shows the temperature dependence of some of the stronger reflections. No evidence of any contribution was observed at reciprocal-lattice points with  $l$  even, corresponding to ferromagnetic coupling within the chains.

The interpretation of these results is greatly aided by symmetry considerations. The tripled hexagonal magnetic cell with dimensions  $a\sqrt{3}$ ,  $c$  is shown in Fig. 4. From the viewpoint of symmetry, there are two logical ways of constructing this cell from the parent  $P6_3/mmc$  cell. In the first of these, the new origin coincides with the old on the  $6_3$  axis, and there are two inequivalent sets of Co sites. Alternatively, the new origin can be placed on the  $\bar{6}$  axis, but in this case there is only one type of Co site and the collinear ferromagnetic basal plane arrangement of Fig. 5(b) is not allowed by symmetry, i.e., the only collinear arrangements in the plane which are allowed are

ferromagnetic. We therefore restrict ourselves to the first choice of cell.

The highest symmetry subgroup in this case is  $P6_3/mcm$ . The Co site-I ions are on the 2 (b) sites at 000,  $00\frac{1}{2}$  and the Co site-II ions are on 4 (*d*) sites at  $\frac{1}{3}\frac{2}{3}0$ ,  $\frac{2}{3}\frac{1}{3}0$ ,  $\frac{1}{3}\frac{2}{3}\frac{1}{2}$ , and  $\frac{2}{3}\frac{1}{3}\frac{1}{2}$ . In all cases,  $c$ -axis nearest neighbors are assumed to be antiferromagnetically coupled. Reference to magnetic-space-group tables<sup>10</sup> reveals that two basic arrangements are allowed within a given basal plane, designated *A* and *B* (Fig. 7). The first of these has magnetic symmetry  $P6_3/m'cm$ , and the moments on the site-II ions are coupled antiparallel along the  $c$  axis. However, symmetry does not permit an ordered moment on the site-I ion. In structure *B* with magnetic symmetry  $P6_3'/m'cm'$ , the moments on site II are parallel, and in this case a moment is allowed on site I. This is not required to have the same value as those on the site-II ions, and may lie either parallel or antiparallel with respect to the latter. We shall be interested mainly in the antiparallel case. The structure factors per magnetic unit cell for (*hhl*) reflections with  $l$  odd corresponding to these structures are

$$A: F = i4\mu_{II}(\sin 2\pi h) \times 0.2695f \quad (1a)$$

$$B: F = 2[\mu_I + 2\mu_{II}\cos 2\pi h] \times 0.2695f, \quad (1b)$$

where  $f$  is the magnetic form factor (assumed to be the same for both types of ion) and  $\mu_I$  and  $\mu_{II}$  the respective moments.

For structure *A*, reflections of the type (*hhl*) are absent for integral  $h$  [e.g., (111)], whereas such reflections will generally be present for the *B* structure, except in the special case where  $\mu_{II} = -\frac{1}{2}\mu_I$  (*C* structure, Fig. 7) in which case the structure factors for these two models are identical apart from a multiplicative factor of  $2/\sqrt{3}$ . This

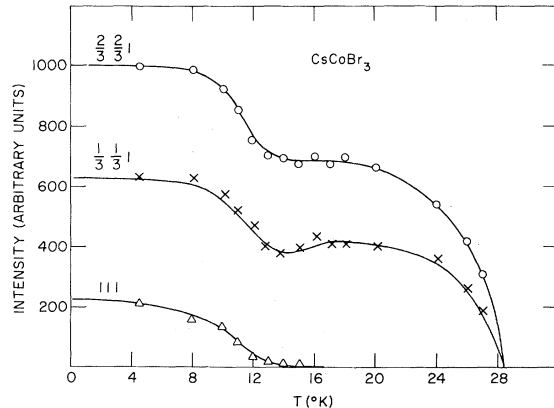


FIG. 6. Temperature dependence of some of the strong reflections in CsCoBr<sub>3</sub>. Note disappearance of (111) intensity at about 14°K.

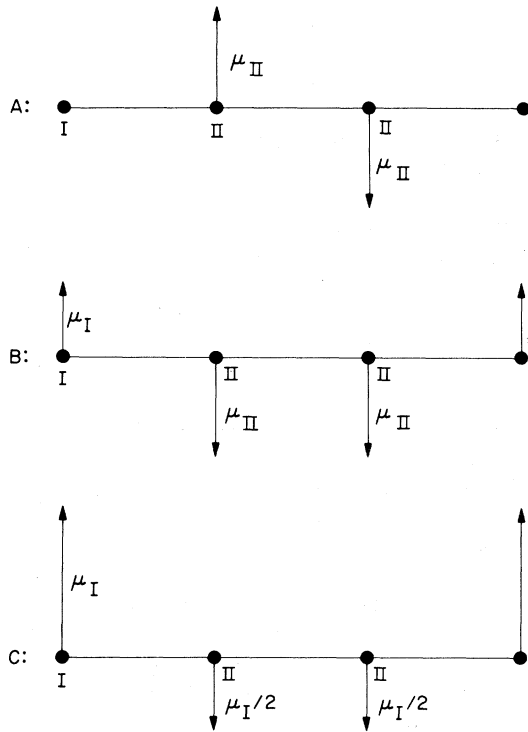


FIG. 7. Basic structure derived from tripled cell: (a) *A* mode with disorder on site I; (b) *B* mode with  $\mu_I$  and  $\mu_{II}$  arbitrary; (c) *C* mode, special case of *B* for which  $\mu_{II} = -\frac{1}{2}\mu_I$ .

type of degeneracy turns out to be a common feature in these systems and often more than one model will give the same fit to the experimental data. Frequently, simple symmetry arguments are not sufficient to choose between models. For example, both model *A* and model *C* are sinusoidal modulations of the basic hexagonal cell by a  $\vec{k}$  vector  $(\frac{1}{3}, \frac{1}{3}, 0)$ , with a phase difference of  $\pi/2$ , and one cannot be chosen in preference to the other by symmetry arguments alone. It is therefore necessary to consider other experimental evidence before making a choice of model.

The triangular type of structure observed in CsNiCl<sub>3</sub> cannot be explained on the above basis, however, since the magnetic space groups based on  $P6_3/mcm$  and their hexagonal subgroups require that the magnetic moments in the Co special positions lie along the *c* axis. In general, therefore, lower-symmetry models must be considered. Detailed consideration of the intensities of the strongest magnetic reflections indicate that some deviation of the spin direction from the *c* axis must also occur in CsCoBr<sub>3</sub> as a function of temperature. In particular, the ratio of  $I(\frac{1}{3}, \frac{1}{3}, 1) : I(\frac{2}{3}, \frac{2}{3}, 1)$  has a minimum at about 14 °K and is significantly larger at either 4 or 20 °K (Fig. 6). Extinction effects seem to be ruled out as the source of this varia-

tion, since in that case one would expect the stronger reflection to be most affected, such that the above ratio would decrease monotonically with the degree of order, and hence with the temperature.

### C. Lower symmetry models

The highest symmetry structures with nonaxial moments, consistent with the observed reflections, are orthorhombic. The appropriate *C*-centered cell is illustrated in Fig. 4 and has dimensions  $3a, a\sqrt{3}, c$ . A systematic search of the space group tables<sup>10</sup> yields a number of possible magnetic structures with antiferromagnetic coupling along the *c*-axis chains and an allowed basal plane component.<sup>11</sup> One of these possibilities is a combination of the *A<sub>z</sub>* and *B<sub>x</sub>* modes which has  $Cmc2_1$  symmetry, and another is a combination of *B<sub>z</sub>* and *A<sub>x</sub>* modes with  $Cm'c2'_1$  symmetry.<sup>11</sup> The orthorhombic structures *A<sub>z</sub>B<sub>y</sub>* and *B<sub>z</sub>A<sub>y</sub>* can also be obtained ( $C22_1$  and  $C2'2'_1$ , respectively), but the symmetry of structures such as *A<sub>x</sub>A<sub>z</sub>*, a nonaxial collinear structure, is monoclinic ( $C2'/c$ ), as is the *B<sub>x</sub>B<sub>z</sub>* structure ( $C2/c$ ).

The ideal triangular structure can then be described as a combination of *B<sub>z</sub>* and *A<sub>x</sub>* (or *A<sub>y</sub>*) modes with  $|\mu_I| = |\mu_{II}| = \mu$ , with  $\mu_I$  directed along the *c* axis and  $\mu_{II}$  120° away [Fig. 5(c)]. The corresponding structure factors are

$$F_{11} = 2 \times 0.2695 f \times \mu (1 - 2 \cos 60 \cos 2\pi h), \quad (2a)$$

$$F_{1-1} = i 2 \times 0.2695 f \times \mu (-2 \sin 60 \sin 2\pi h). \quad (2b)$$

From the relationships given in Fig. 5, it is clear that the appearance of the (111) reflection below 14 °K must reflect the presence of a predominantly *B*-type mode, and rough intensity calculations at 4.4 °K show that reasonable agreement is obtained for a *B<sub>z</sub>* structure [Fig. 5(b)] in which  $\mu_I = -\mu_{II} \approx 3\mu_B$ , as was found in RbCoBr<sub>3</sub>,<sup>7</sup> and was also reported for the low-temperature structure of CsCoCl<sub>3</sub>.<sup>5</sup> However, fits of the data indicate that the structure of CsCoBr<sub>3</sub> is not axial.<sup>12</sup>

We now have two possible models to describe the gradual disappearance of the (111) intensity as the temperature is increased. One model requires that, first of all,  $\mu_{II}$  disorder more rapidly than  $\mu_I$ , and then become approximately equal to  $-\frac{1}{2}\mu_I$  at 14 °K and above [see Eq. (1b)]. However, not only does this seem a rather artificial model, but also, to account for the observed intensities, it is necessary for  $\mu_I$  to increase as the temperature is raised, up to a value of about  $3.5\mu_B$  at 14 °K. This seems quite unlikely.

A more plausible explanation is that the *B<sub>z</sub>* structure gradually transforms, in the 10–14 °K temperature range, to the *A<sub>z</sub>* structure, in which the Co site-I chains of moments are completely

disordered with respect to coupling in the basal plane while the Co site-II chains retain an ordered arrangement with moments of about  $3\mu_B$ . This disorder is not complete in three dimensions. One would expect, given the one-dimensional nature of the material, that the correlations remain extremely long-range along the  $c$  axis. What is lost are the correlations *between* the site-I chains, so that on the average half would be up-down-up, and the other half would be down-up-down. This is energetically quite reasonable; it is clear that if the moments on two of the sites are axial and antiparallel, then it is irrelevant whether the spin on the third site is up or down; the average energy is the same. If long-range  $c$ -axis correlations persist in the antiferromagnetic chains, very little energy will be lost in the disordering process. It is perhaps significant in this regard that the disordering occurs in the temperature range for which the fitting procedure gives a minimum in the canting. It should be possible to confirm this model directly in a crystal of suitable size by a study of the diffuse scattering. Such uncorrelated  $c$ -axis chains should produce "sheets" of diffuse scattering perpendicular to  $c^*$ , as is observed above  $T_N$  in several related compounds. We might expect that in  $\text{CsCoBr}_3$  these sheets would persist between  $14^\circ\text{K}$  and  $T_N$ , with roughly one-third of the intensity observed just above  $T_N$ .

The change of structure could be a discontinuous process involving a change in symmetry from  $P6_3'/m'cm'$  to  $P6_3/m'cm$  (or in the more general case, the corresponding orthorhombic subgroups), and the two phases would coexist in this intermediate range. Alternatively, a continuous process could be envisaged in which one-half of the Co site-II chains in the  $B_x$  structure gradually disorder. This requires a lowering of the symmetry to monoclinic in the intermediate range, since it requires three inequivalent cobalt sites. For simplicity, the detailed analysis of the magnetic data described in Sec. V has been based on the high symmetry two-phase orthorhombic model, including small basal-plane components where appropriate. It should be emphasized, however, that identical neutron intensities can be derived from either model and that the two-phase model may be thought of, in one sense, as a separation of a monoclinic structure into two components.

#### V. DETAILED MAGNETIC STRUCTURE REFINEMENT

The intensities of thirteen magnetic peaks were measured at several temperatures, while a more limited data set of seven peaks was obtained at a few intermediate points. Equivalent peaks were found to agree to within (5–10)%. Average values of the instrumental scale factor, temperature factor, and extinction parameter were determined from

the nuclear structure refinements and held constant for the magnetic structure analysis. The theoretical Freeman-Watson form factors<sup>13</sup> for  $\text{Co}^{2+}$  were used, modified by a scaling constant of the type  $f' = f(k\sin\theta/\lambda)$  to allow for expansion or contraction of the spin density.

A number of factors must be considered in these refinements. For example, the effect of allowing a component of the moment to lie perpendicular to the  $c$  axis is to increase the intensity of the reflections closest to the  $c$  axis relative to those further away. Unfortunately, the form-factor scaling parameter  $k$  acts in much the same way for most of the strong peaks, and as a result, not only were the resulting correlation coefficients and standard errors quite high, but also the values of  $k$  obtained varied considerably, from 0.75 to 0.95. The assumption was therefore made that the  $14^\circ\text{K}$  data represent a collinear  $A_x$  arrangement with no perpendicular component, since in this case the ratio of the intensity  $I(\frac{1}{3}\frac{1}{3}1)$  to those of the other peaks is a minimum. On this basis, the refinement gave a satisfactory fit to the data with a  $k$  value of 0.824, and  $k$  was held at this value for the other refinements. This expansion is comparable to that observed for  $\text{Ni}^{2+}$  in similar environments.<sup>4,14</sup> Although this procedure is admittedly somewhat arbitrary, the essential conclusions remain the same for any value of  $k$  between 0.8 and 0.9.

The data above  $14^\circ\text{K}$  were fitted to the  $A_x B_x$  model ( $Cmc2_1$ ) and those at  $4^\circ\text{K}$  to the  $B_x A_x$  structure ( $Cm'c2_1'$ ), although the  $A_x B_y$  and  $B_x A_y$  models would of course give identical results. In the intermediate region the data were fitted to a two-phase model in which both structures were assumed to coexist. However, the calculated intensity expressions are of such a form as to give a singularity in the refinement when all the parameters were varied. We have therefore assumed that the  $B_x$  component is zero in the two-phase region from about  $10$  to  $14^\circ\text{K}$  and that the system is a mixture of  $B_x A_x$  and  $A_x$  structures, i. e., the perpendicular component is only present in the low-temperature phase. We have also assumed that at a given temperature the magnitude  $\mu$  of the  $\text{Co}^{2+}$  moment on every ordered site is the same in both structures. This moment, the basal-plane component (expressed in terms of the canting angle  $\theta$ ) in the low-temperature  $B_x A_x$  phase, and the fraction of the  $A_x$  phase [which depends sensitively on the (111) intensity] were therefore the parameters varied in this temperature region.

At  $4.5^\circ\text{K}$  the data were fitted satisfactorily to a  $B_x A_x$  structure alone with  $\mu_{1x}$  antiparallel to  $\mu_{11x}$ ,  $\mu = (3.02 \pm 0.03)\mu_B$ , and  $\theta = 9.7^\circ \pm 1.5^\circ$  corresponding to a basal-plane component of about  $0.5\mu_B$ . Above  $14^\circ\text{K}$ , any contribution to the (111) intensity has been attributed to the  $B_x$  component. At  $16^\circ\text{K}$

TABLE III. Parameter values obtained from the least-squares analyses of the magnetic data from CsCoBr<sub>3</sub> at the six temperatures studied. Form-factor scaling constant  $k$  was fitted at 14°K and held fixed at 0.824 at all other temperatures.

	4.5°K	10°K	11°K	14°K	16°K	20°K
Total Co <sup>2+</sup> moment	3.02(3)	2.90(5)	3.02(3)	2.95(3)	3.01(2)	2.88(2)
Component in basal plane on site II ( $B_x A_x$ )	0.51(8)	0.90(9)	0.60(8)	0.0	...	...
Component in basal plane on site I ( $A_x B_x$ )	...	...	...	...	0.12(18)	0.36(8)
Fraction $A_x B_x$ structure	0.0	0.16(7)	0.55(2)	0.92(1)	1.0	1.0
Number of reflections	13	7	13	7	13	13
$R_w$	0.093	0.065	0.059	0.043	0.051	0.048

the canting is zero within the standard error, but at 20°K the fitting procedure yields a significant basal-plane component of  $0.4\mu_B$ .

The results of the least-squares refinement are summarized in detail in Table III, and in Table IV we give the observed and calculated magnetic intensities at 4.5 and 20°K. It is to be noted that the moment per Co<sup>2+</sup> ion has the reasonable value of about  $3\mu_B$ , and that within experimental error, there are no discontinuities over the temperature range studied (Fig. 8).

TABLE IV. Comparison of observed and calculated single-crystal magnetic intensities for the highest and lowest temperatures studies in detail, i. e., 4.5 and 20°K. Parameters as in Table III. n. o. denotes "not observed."

$hkl$	4.5°K		20°K	
	$I_{obs}$	$I_{calc}$	$I_{obs}$	$I_{calc}$
001	0.02	0.0	n. o.	0.0
$\frac{1}{3}\frac{1}{3}1$	6.4	6.0	4.2	4.1
$\frac{2}{3}\frac{2}{3}1$	10.2	9.2	6.8	6.5
111	2.1	2.6	0.04	0.05
$\frac{4}{3}\frac{4}{3}1$	6.6	6.4	4.4	4.5
$\frac{5}{3}\frac{5}{3}1$	4.6	4.6	3.3	3.3
221	0.70	0.8	0.02	0.02
$\frac{7}{3}\frac{7}{3}1$	2.0	2.3	1.5	1.6
$\frac{1}{3}\frac{1}{3}3$	0.18	0.28	0.13	0.16
$\frac{2}{3}\frac{2}{3}3$	0.64	0.65	0.35	0.42
113	0.21	0.22	n. o.	0.05
$\frac{4}{3}\frac{4}{3}3$	1.2	1.1	0.88	0.78
223	0.23	0.24	n. o.	0.005
331	0.20	0.24	n. o.	0.005

The single-crystal results are quite compatible with the powder data, although the latter were neither extensive nor accurate enough to permit a systematic analysis of this sort to be carried out. However, the presence of the additional set of orthorhombic peaks in the powder data deserves further comment. The structures determined from the single-crystal data are shown in Figs. 9(a) and 9(b). In Fig. 9(c) a possible structure for the orthorhombic cell is illustrated. This is now based on the  $3a, a\sqrt{3}, c$  cell rather than the  $a\sqrt{3}, a, c$  cell of Fig. 4, and has symmetry  $C_P m' c 2'_1$ . The transition in the powder would therefore be from  $Cmc2_1$  to a mixture of  $Cm' c 2'_1$  and  $C_P m' c 2'_1$ .

Examination of these three structures shows that each cobalt ion has an average of two antiparallel near neighbors in the basal plane. The  $Cm' c 2'_1$  and  $Cmc2_1$  structures would be favored if the next-nearest-neighbor exchange in the basal plane were positive while the  $C_P m' c 2'_1$  structure is favored by negative second-neighbor exchange. Since the next-nearest-neighbor distance is about 13 Å, this interaction is

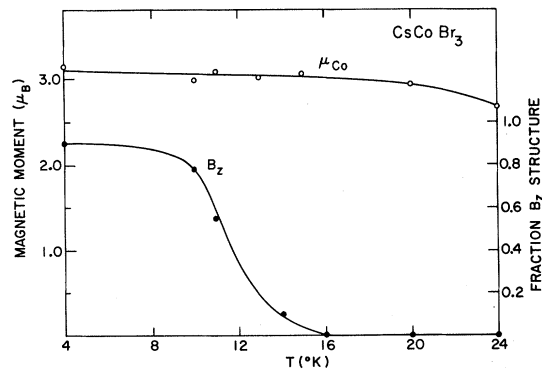


FIG. 8. Temperature dependence of the fitted Co moment and fraction of structure  $B_x A_x$  present, as derived from the fitting procedure.

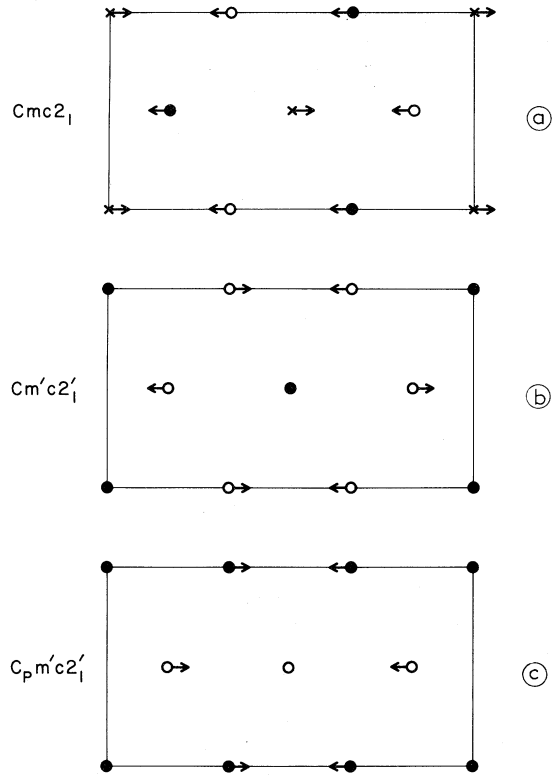


FIG. 9. Final orthorhombic models for CsCoBr<sub>3</sub>. Arrows indicate in-plane components, solid and open circles indicate moments into and out of the plane respectively, while crosses indicate disordered axial components of the moment. (a) High-temperature structure. (b) Low-temperature structure observed for the single crystal. (c) Low-temperature structure characterized by powder peaks of type *m'* in Fig. 3.

expected to be quite weak and may be sensitively affected by impurities, etc. The same situation will not arise for the high-temperature *Cmc2<sub>1</sub>* phase since the related *P* cell will have an average

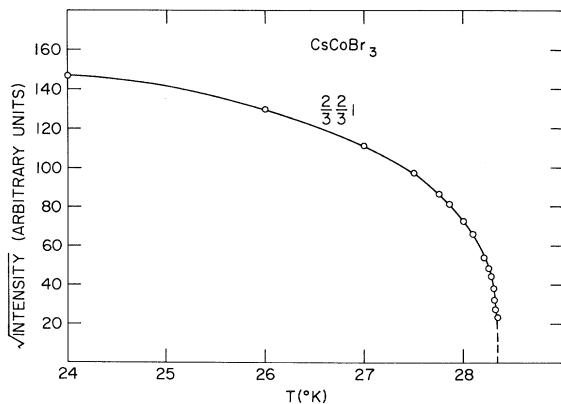


FIG. 10. Temperature dependence of the  $(\frac{2}{3} \frac{2}{3} 1)$  reflection close to  $T_N$ .

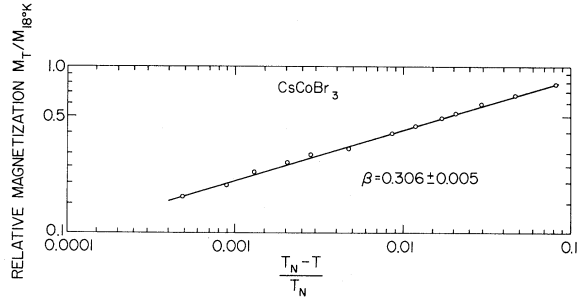


FIG. 11. Log-log plot of the relative magnetization as a function of reduced temperature.  $\beta$  is typical of a three-dimensional Ising lattice.

of only  $\frac{2}{3}$  antiparallel neighbors, and the two structures will be energetically quite different. The coexistence of two phases differing only in the coupling between very distant neighbors has been observed in the two-dimensional antiferromagnets Rb<sub>2</sub>MnF<sub>4</sub><sup>15</sup> and BaCoF<sub>4</sub>.<sup>16</sup>

## VI. MAGNETIZATION OF CsCoBr<sub>2</sub> IN THE CRITICAL REGION

Within the precision of our measurements, no change in the relative intensities of the magnetic reflections could be observed above 24 °K, indicating that the canting angle had become constant. The intensities therefore provide a direct measure of the magnetization, and the intensity of the  $(\frac{2}{3} \frac{2}{3} 1)$  peak as a function of temperature is shown in Fig. 10. The magnetization  $\{M \propto [I(\frac{2}{3} \frac{2}{3} 1)]^{1/2}\}$  was fitted between 26 and 28.32 °K to the expression  $M = A[(T_N - T)/T_N]^\beta$ .

The data can be fitted very well with the values  $\beta = 0.306 \pm 0.005$  (Fig. 11) and  $T_N = 28.334 \pm 0.002$  °K (relative errors). The value for  $T_N$  agrees very well with the independent figure of  $28.338 \pm 0.004$  °K obtained from the peak in the critical scattering. Consideration of the systematic errors yield the following final values of the parameters:  $\beta = 0.31 \pm 0.01$ ,  $T_N = 28.34 \pm 0.05$ .

These results agree well with the prediction of the three-dimensional Ising model<sup>17</sup> for which  $\beta = 0.3125$ , and indicate that despite the predominantly one-dimensional nature of the structure and magnetic susceptibility, the ordering is characteristically three dimensional. Similar results have been obtained for RbNiCl<sub>3</sub>,<sup>4</sup> but  $\beta$  is significantly different for CsNiF<sub>3</sub> in a similar reduced temperature interval.<sup>9</sup>

## VII. DISCUSSION

The above measurements show that two magnetic transitions occur in CsCoBr<sub>3</sub>. The transition from the paramagnetic phase which occurs at about 28 °K is rather unusual in that only two-thirds of the chemically equivalent Co moments appear to order, the remaining one-third ordering only be-



low about 10 °K. However, although the general features of the magnetic ordering of CsCoBr<sub>3</sub> are clear, certain problems require further study. The space groups proposed for the ordered structures cannot be derived from the paramagnetic group by a modulation by a single  $k$  vector, an apparent violation of Landau's theory of second-order phase transitions.<sup>18</sup> It has been pointed out, however, that this criterion should apply only in the immediate vicinity of the phase transition, and that far from  $T_N$  one may see further lowering of the symmetry occurring in a continuous manner.<sup>19</sup> As was pointed out earlier,<sup>12</sup> a collinear structure in the low-temperature phase will be unstable to some canting and thus an orthorhombic structure might be expected.

Over the entire range of temperatures, the direction of the basal-plane component cannot be determined. The choice between  $A_x B_z$  or  $A_y B_z$

models is purely arbitrary, and the data do not rule out the possibility of a general direction for the basal-plane spin component. Likewise, in the intermediate range 10–14 °K, it is not clear whether the symmetry change is continuous or discontinuous. The specific-heat data show that any entropy involved in this transition is very small, but this is hardly surprising since antiferromagnetic correlations within the chains must be long range in this temperature region, and the remaining disorder is small.

#### ACKNOWLEDGMENTS

We are grateful to F. S. L. Hsu for performing the specific-heat measurements, and to J. V. Waszczak for the magnetic measurements. Helpful discussions with V. J. Minkiewicz are also acknowledged.

\*Work performed at Brookhaven National Laboratory, under the auspices of the Energy Research and Development Administration.

†Formerly at Brookhaven National Laboratory, Upton, N. Y. 11973.

<sup>1</sup>N. Achiwa, *J. Phys. Soc. Jpn.* **27**, 561 (1969); also see the review articles: L. J. de Jongh and A. R. Miedema, *Adv. Phys.* **23**, 1 (1974); J. F. Ackerman, G. M. Cole and S. L. Holt, *Acta Chim Inorg.* **8**, 323 (1974).

<sup>2</sup>D. E. Cox and V. J. Minkiewicz, *Phys. Rev. B* **4**, 2209 (1971).

<sup>3</sup>V. J. Minkiewicz, D. E. Cox, and G. Shirane, *Solid State Commun.* **8**, 1001 (1970).

<sup>4</sup>W. B. Yelon and D. E. Cox, *Phys. Rev. B* **6**, 204 (1972).

<sup>5</sup>M. Melamud, H. Pinto, J. Makovsky, and H. Shaked, *Phys. Status Solidi* **63**, 699 (1974).

<sup>6</sup>D. E. Cox and F. C. Merkert, *J. Cryst. Growth* **13/14**, 282 (1972).

<sup>7</sup>In view of the various different cells to be referred to, we have consistently used fractional indices based on the hexagonal paramagnetic cell.

<sup>8</sup>V. J. Minkiewicz, D. E. Cox, and G. Shirane, *J. Phys. (Paris) C* **1**, C-892 (1971).

<sup>9</sup>M. Steiner, *Solid State Commun.* **11**, 73 (1972).

<sup>10</sup>W. Opechowski and R. Guccione, *Magnetism*, edited by G. T. Rado and H. Shal (Academic, New York 1965) Vol. II A, Chap. 3.

<sup>11</sup>In Ref. 5, our space-group assignments were incorrect-

ly referred to in terms of the higher-symmetry hexagonal space groups rather than the orthorhombic groups given here and previously [see W. B. Yelon, D. E. Cox, and V. J. Minkiewicz, *Bull. Amer. Phys. Soc.* **17**, 339 (1972)].

<sup>12</sup>The collinear  $B_z$  structure with equal moments and isotropic exchange is not a stable structure since the in-plane exchange will cancel exactly on the site-II cobalt ions. Some canting should occur to stabilize the structure. Anisotropic exchange and higher-order terms in the anisotropy may also play a role in these compounds, but these would also be expected to favor some form of canting. It is therefore probable that all of the three compounds CsCoBr<sub>3</sub>, CsCoCl<sub>3</sub> (Ref. 5) and RbCoBr<sub>3</sub> (Ref. 8) are nonaxial and have orthorhombic symmetry.

<sup>13</sup>R. E. Watson and A. J. Freeman, *Acta Crystallogr.* **14**, 27 (1961).

<sup>14</sup>W. B. Yelon and D. E. Cox, *Phys. Rev. B* **7**, 2024 (1973).

<sup>15</sup>R. J. Birgeneau, H. J. Guggenheim, and G. Shirane, *Phys. Rev. B* **1**, 2211 (1970).

<sup>16</sup>M. Eibschütz, L. Holmes, H. J. Guggenheim, and D. E. Cox, *Phys. Rev. B* **6**, 2677 (1972).

<sup>17</sup>G. A. Baker and D. S. Gaunt, *Phys. Rev.* **155**, 545 (1967).

<sup>18</sup>L. D. Landau and E. M. Lifshitz, *Statistical Physics* (Addison-Wesley, Reading, Mass., 1958), Chap. 14.

<sup>19</sup>J. O. Dimmock, *Phys. Rev.* **130**, 1337 (1963).